PHYSICAL REVIEW A VOLUME 8, NUMBER 6 DECEMBER 1973

Kinetic Theory of Collisional Line Narrowing in Pressurized Hydrogen Gas*

S. H. Chen, Y. Lefevre, and S. Yip
Nuclear Engineering Department, Massachusetts Institute of Technology, Cambridge, Massachusetts 02139
(Received 29 June 1973)

We measure the incoherent quasielastic scattering of thermal neutrons from hydrogen gas at 85°K and various pressures up to 140 atm. The observed Van Hove self-correlation function (or the self-part of the dynamic structure factor) shows a narrowing effect as the ratio of the observational wavelength to the collisional mean free path increases. The resulting line shape and linewidths are analyzed using an appropriate kinetic equation. The theoretical prediction agrees with experiment when the only parameter in the theory, namely, the self-diffusion coefficient, is properly calculated in the Enskog approximation. We demonstrate experimentally that the linearized Boltzmann equation gives an accurate description of the dynamics of the single-particle motion at moderately high density and in the range of wave vectors and frequencies comparable to inverse collision mean free paths and collision frequencies of the molecules.

I. INTRODUCTION

Kinetic equations, formulated as a well-posed initial-value problem, provide perhaps the most systematic method of evaluating classical time correlation functions.[1] This approach has several advantages. It allows a molecular treatment of the collisions among particles, especially those involving only two molecules at a time. It gives the proper macroscopic behavior of time correlation functions when general conditions related to conservation laws and hydrodynamics are satisfied. It allows all the thermal fluctuations to be analyzed in a unified calculation since the solution is in terms of the phase-space correlation function. Because of these properties one can regard the kinetic-theory description as an effective interpolation between the microscopic world of intermolecular interactions, mean-field effects, and free molecular flow, on the one hand, and the macroscopic world of transport coefficients and hydrodynamic processes on the other.

For dense gases and liquids the kinetic-theory approach to time correlation functions presents two basic difficulties. The first is that the appropriate collision operators, valid at arbitrary frequencies and wavelengths, have not been available. It is only recently that significant progress in a microscopic derivation of these operators has been made.[2] The second difficulty is the calculation of transport coefficients and thermal fluctuation spectra once the kinetic equations are known.[3] Because of these difficulties recent calculations of time correlation functions in liquids have been carried out either at the level of generalized hydrodynamic equations or involve model collision operators.[1]

In the case of dilute gases the difficulties inherent in a kinetic-theory approach can be largely overcome. It is generally recognized that the kinetic equation which describes the nonequilibrium behavior of a low-density fluid is the linearized Boltzmann equation.[4] This is an intermediate level of description because the collisions are assumed to take place instantaneously between point particles. Since the Navier-Stokes equations of hydrodynamics can be derived from the Boltzmann equation, there is no question that this kinetic equation gives correctly the low-frequency and long-wavelength behavior of time correlation functions. The validity of the Boltzmann equation in the kinetic regime, where wavelengths and frequencies are comparable to collision mean free paths and collision frequencies, can be established on theoretical grounds.[5] Also, recent results from Rayleigh scattering studies[6] and computer molecular-dynamics experiments[7] support this view. However, at still higher frequencies and shorter wavelengths one can expect the Boltzmann equation to break down. When the frequencies become comparable to the reciprocal of the collision duration and wavelengths become comparable to the particle diameter, one can intuitively see that any collision operator which treats the interaction as an instantaneous collision between two point particles cannot be valid under these conditions. In order to probe the high-frequency and large-wave-number behavior of correlation functions one needs to consider neutron scattering or computer molecular-dynamics calculations.

Recently a kinetic equation for low-density fluids which is valid for all frequencies and wavelengths has been derived by Mazenko.[8,9] The collision operator, which is explicitly nonlocal

in space and time, has all the desired general properties and reduces in the low-frequency and long-wavelength limit to the Boltzmann collision operator. We will henceforth refer to this equation as the generalized Boltzmann equation. It is interesting to note that the corresponding equation describing the single-particle phase-space correlation function, in the special case of hard-sphere interaction, reduces to the appropriate Boltzmann-Lorentz equation.[10,11] This indicates that in studying the van-Hove self-correlation function in a dilute gas of hard spheres the Boltzmann equation is valid for all frequencies and wavelengths.

In order to experimentally test the validity of the above statement we carried out a quasielastic neutron scattering experiment on hydrogen gas at 85°K. Since hydrogen is predominantly an incoherent scatterer the measured cross section is proportional to the self-part of the dynamic structure factor, which can be calculated from the single-particle phase-space correlation function, as will be done in Sec. II. Our preliminary experimental results were reported in Ref. 12, where we showed that the qualitative feature of the line narrowing with the increase in pressure can be accounted for by the one-relaxation-time kinetic model of Nelkin and Ghatak.[13] We have since then carried out a more extensive measurement at various pressures and we shall carefully study the linewidth by using the rigorous solution of the Boltzmann equation in the special case of a hard-sphere gas. There is good evidence[14] that the linewidth of the van-Hove self-correlation function is insensitive to the details of the intermolecular potential function, except for its equivalent hard-sphere diameter. Although according to Mazenko et al.[10] the Boltzmann equation is valid for all frequencies and wavelengths only at low densities, i.e., $\eta \equiv \frac{1}{6}\pi n r_0^3 < 0.005$, where n is the number density and r_0 the equivalent hard-sphere diameter, we shall show that the result can be greatly extended to high densities provided that the Enskog correction is made to the self-diffusion coefficient. The experiment also shows that the scaling property of the Boltzmann equation, namely, that the reduced linewidths vs the dimensionless parameter y is a universal function, is well obeyed up to a density $\eta = 0.13$, which is significantly larger than 0.005 and is close to the critical density of hydrogen.

The significance of our experiment lies in the fact that it, for the first time, experimentally establishes the validity of the linearized Boltzmann equation in describing the single-particle motion in a dense gas in the distance and time scale of the order of the mean free path and the mean collisional time of the molecules.

II. KINETIC THEORY

The fundamental quantity in the kinetic-theory description of thermal fluctuations in gases and liquids is the time-dependent phase-space density correlation function.[1] The analogous function in the test-particle problem (self-correlation) is

$$S_s(\vec{r}-\vec{r}', \vec{p}\vec{p}', t-t') = (1/n)\langle \delta f_s(\vec{r}\vec{p}t)\delta f_s(\vec{r}'\vec{p}'t')\rangle , \tag{1}$$

where

$$f_s(\vec{r}\vec{p}t) = \sqrt{N}\delta(\vec{r}-\vec{R}(t))\delta(\vec{p}-\vec{P}(t)) \tag{2}$$

is the single-particle phase-space density, and δf_s is the deviation of f_s from its equilibrium value $\langle f_s\rangle = n f_0(p)/\sqrt{N}$. The position and momentum of the test particle are denoted by $\vec{R}(t)$ and $\vec{P}(t)$. There are N particles in the fluid system of volume Ω, so the average density is $n = N/\Omega$. The angular brackets denote an average over an equilibrium ensemble, and

$$f_0(p) = (\beta/2\pi m)^{3/2} e^{-\beta p^2/2m} \tag{3}$$

is the normalized Maxwellian momentum distribution at temparature $T = (\beta k_B)^{-1}$ for particles with mass m. We see that $\langle f_s\rangle$ vanishes in the thermodynamic limit so S_s is the autocorrelation function of f_s.

We consider only classical fluids which are invariant to spatial and time translations, rotations, and inversions. Then the spatial and time dependence of the correlation function appears only through the magnitude of $\vec{r}-\vec{r}'$ and the time difference $t-t'$. At $t=t'$, S_s assumes its static value

$$S_s(r, \vec{p}\vec{p}', 0) = f_0(p)\delta(\vec{p}-\vec{p}')\delta(r) . \tag{4}$$

In the following calculations we will deal directly with the Fourier-Laplace transform of (1):

$$S_s(k\vec{p}\vec{p}'z) = -i\int_0^\infty dt\, e^{izt} \times \int d^3r\, e^{-\vec{k}\cdot\vec{r}} S_s(r, \vec{p}\vec{p}', t) , \tag{5}$$

where z is a complex frequency $z = \omega + i\epsilon$, with ϵ small and positive. One can show that $S_s(k\vec{p}\vec{p}'z)$ satisfies a kinetic equation of the form[15]

$$(z - \vec{k}\cdot\vec{p}/m)S_s(k\vec{p}\vec{p}'z) = J_s[S_s] + \bar{S}(k\vec{p}\vec{p}') , \tag{6}$$

where the initial condition $\bar{S}_s$ is the spatial Fourier transform of (4), and $J_s[S_s]$ expresses the collisional effects. It is useful to write

$$J_s[S_s] = \int d^3p''\, \varphi_s(k\vec{p}\vec{p}''z)\, S_s(k\vec{p}''\vec{p}'z) , \tag{7}$$

thus introducing a space- and time-dependent collision kernel often referred to as the memory function.

The calculation of $\varphi_s(k\vec{p}\vec{p}'z)$ for dense gases and liquids is a complicated problem of considerable theoretical interest[2] but will not be discussed here. In the case of dilute gases general expressions for φ_s and the corresponding memory function for density fluctuations have been derived recently by Mazenko.[8] These results show that for an arbitrary intermolecular potential, $\varphi_s(k\vec{p}\vec{p}'z)$ depends only on the dynamics of binary collisions and is, in general, frequency and wave-number dependent; however, in the special case of hard-sphere interaction, φ_s becomes independent of both z and k.[10,11] For this case the collisional integral is

$$J_s[S_s] = in r_0^2 \int d^3p_1\, d\Omega_r \frac{\hat{r}\cdot(\vec{p}-\vec{p}_1)}{m}\Theta_-(\hat{r}\cdot(\vec{p}-\vec{p}_1)) \times[f_0(p_1)S_s(k\vec{p}\vec{p}'z) - f_0(p_1^*)S_s(k\vec{p}^*\vec{p}'z)], \quad (8)$$

where r_0 is the hard-sphere diameter, $\Theta_-(x)$ is the step function (unity where $x<0$ and zero otherwise), and the asterisk denotes the post-collision momentum variable. When (8) is inserted into (6) one finds that the kinetic equation is precisely the linearized Boltzmann equation for the test-particle problem with hard-sphere interactions. This is the only known case where the Boltzmann-equation solutions are valid at arbitrary frequencies and wavelengths.

Equation (6) with J_s given by (8) has been studied by Mazenko, Wei, and Yip.[10] Their numerical results, along with other calculations using the Boltzmann equation, will be discussed later in Sec. V. For the purpose of analyzing incoherent-neutron-scattering data one is interested in the van-Hove self-correlation function[16]

$$G_s(r,t) = \Omega\langle\delta(\vec{r}-\vec{R}(t))\delta(\vec{R}_1)\rangle \quad (9)$$

or, rather, its transform

$$S_s(k\omega) = \int_{-\infty}^{\infty}\frac{dt}{2\pi}\int d^3r\, e^{-i(\vec{k}\cdot\vec{r}-\omega t)}G_s(r,t), \quad (10)$$

where ω is a real frequency. The latter can be obtained directly from the kinetic equation solutions as

$$S_s(k\omega) = -\frac{1}{\pi}\,\mathrm{Im}\left[\int d^3p\, d^3p'\, S_s(k\vec{p}\vec{p}'z)\right]_{z=\omega+i\epsilon}. \quad (11)$$

While the detailed behavior of $S_s(k\omega)$ for any intermolecular potential can be obtained only by numerical calculations, its asymptotic properties are well known.[13] It is convenient to introduce a collision parameter y defined as $\alpha/\sqrt{2}kv_0$, where α is a typical collision frequency and $v_0 = (k_BT/m)^{1/2}$ is the thermal speed. The dimensionless parameter y is then a measure of the ratio of the wavelength of fluctuations to the collision mean free path. In the limit of small y we expect $S_s(k\omega)$ to have a Gaussian form,

$$S_s(k\omega) = (\sqrt{\pi}kv_0)^{-1}e^{-\omega^2/k^2v_0^2}, \quad y \ll 1 \quad (12)$$

which is the line-shape characteristic of Doppler broadening. At the opposite extreme of large y, $S_s(k\omega)$ should have a Lorentzian form,

$$S_s(k\omega) = \frac{1}{\pi}\frac{Dk^2}{\omega^2+(Dk^2)^2}, \quad y \gg 1 \quad (13)$$

the line shape describing diffusive motions. In (13) D is the self-diffusion coefficient.

Any solution of (6) will have the correct limiting behavior (12) and also (13) provided the collision operator does not violate the property of particle-number conservation. The distinction between the Boltzmann-equation solutions with different interaction potentials, or even between a Boltzmann-equation solution and an approximate calculation, is therefore a matter of the behavior of $S_s(k\omega)$ in the intermediate region where $y\sim 1$. One can avoid the complexity of solving the Boltzmann equation by using suitable kinetic models. The first model introduced in this context is the single-relaxation-time kinetic model.[13] The memory function corresponding to this model is simply

$$\varphi_s(k\vec{p}\vec{p}'z) = -i\alpha[\delta(\vec{p}'-\vec{p}) - f_0(p)], \quad (14)$$

where α is an appropriate collision frequency. Equation (14) leads to a simple kinetic equation which allows $S_s(k\omega)$ to be expressed in terms of tabulated functions. We will see later that the results of such a model are only qualitatively useful in interpreting neutron scattering data.[12]

III. NEUTRON SCATTERING FROM HYDROGEN

The low-energy neutron scattering cross section of hydrogen molecules can be expressed in terms of contributions corresponding to definite rotational transitions.[17,18] At a temperature of 85 °K, the sample temperature of our experiment, we need only consider the $J=0$ (para) and $J=1$ (ortho) states since population of the $J\geq 2$ levels is negligible. Even though parahydrogen scattering is purely coherent we can neglect it because the orthohydrogen cross section is predominantly incoherent and is some 30 times that of the parahydrogen. If we further restrict our measurement and analysis to the quasielastic region of the scattering, we can also neglect the $1\to 0$ transition because of the presence of a form factor $j_1^2(Qb)$, where j_1 is the first-order spherical Bessel

function, $2b = 0.75$ Å is the internuclear distance, and $Q \leq 0.6$ Å^{-1} is the wave-number transfer in the experiment. Consequently, the observed line shape may be analyzed in terms of the double-differential cross section[12]

$$\frac{d^2\sigma}{d\Omega\, d\omega} = a_{\text{inc}}^2 N (k/k_0)[j_0^2(Qb) + 2j_2^2(Qb)] \times e^{-\hbar\omega/2k_BT} e^{-\hbar^2Q^2/8mk_BT} S_s(Q,\omega), \quad (15)$$

where a_{inc} is the incoherent scattering length (2.5×10^{-12}cm), k_0 and k are the incident- and scattered-neutron wave number, and $\hbar\omega, \hbar Q$ are the neutron energy and momentum transfers to the sample. The exponential factors appear because we are using a classical time correlation function which does not preserve the property of detailed balance or describe the recoil effects.[19] According to (15) the energy distribution of quasi-elastically scattered neutrons is determined, aside from the known factors, by the spectral distribution of the van-Hove self-correlation function. If we estimate the value of the collision parameter y corresponding to $Q \leq 0.6$ Å^{-1} and gas pressures of about 100 atm at 85 °K, we find that the measurements are in the region of $y \sim 1$. Thus neutron scattering should give a sensitive test of the kinetic-theory predictions.

IV. EXPERIMENTAL DETAILS

A. Description of the Spectrometer

Measurement of the dynamic structure factor $S_s(Q,\omega)$ requires both neutron monochromating and analyzing devices. This can be done by using either a time-of-flight apparatus or a crystal spectrometer, or any combination of the two methods. In this experiment we used a three-axis crystal spectrometer (TAS) located at the MIT reactor (CP-5 type, 5 MW). The TAS used pyrolitic graphite crystals as both the monochromator and the analyzer. It has basically two advantages over the time-of-flight method. First, it can be set to investigate $S_s(Q,\omega)$ in a selected range of Q and ω which is of interest to the experiment. Therefore the information obtained by the spectrometer is never redundant. Secondly, it can be operated in a "constant-Q" mode; that is to say, one can scan through the spectrum of $S_s(Q,\omega)$ at selected Q values. The pyrolitic graphite crystal is an excellent reflector for low-energy neutrons, and furthermore, by selecting the incident neutron energy at $E_0 = 12.6$ meV ($\lambda = 2.55$ Å), we are able to take advantage of an excellent graphite filter (pyrolitic graphite plates stack up to 2-in. length) which removes essentially all the second-order contamination in the incident beam. The monochromatic beam at the sample position is 1 in. high by $\frac{1}{2}$ in. wide, with the total intensity of about 10^7 neutrons/sec. The schematic layout of the spectrometer is shown in Fig. 1. It should be noted that the monochromator section consists of a pair of parallel crystals. This so called "double monochromator" is similar to the original design of Stedman,[20] which offers not only flexibility and ease of the spectrometer design but also possesses some nice features in the energy resolution function. We shall go into the question of resolution function in the following. The experiment was carried out with a fixed incident energy, and energy analysis of the quasielastic peak was made at constant Q ranging in magnitude from 0.2 to 0.6 Å^{-1}. The smallest scattering angle encountered during the runs is 1°.

B. Resolution Function of the TAS

We shall discuss the energy resolution function necessary for extracting the linewidth from the experimental data of the incoherent, quasielastic peak. The complete resolution function of the TAS was studied in great detail in Lefevre's

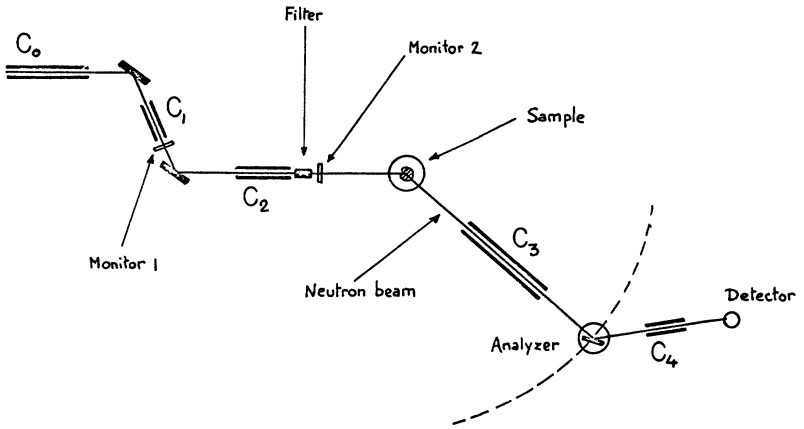

FIG. 1. Schematic arrangement of the MIT three-axis spectrometer. Note the double-monochromator arrangement which makes it slightly unconventional.

thesis,[21] and we shall only quote relevant results applicable to the present experiment. Following Cooper and Nathans[22] we treat the resolution elements, collimators and mosaic crystals, as Gaussian functions with width parameters (standard deviation) α and η. Under normal experimental conditions it is an excellent approximation to treat the vertical resolution as separable from the horizontal resolution.[21] The horizontal resolution determines the line shape and the vertical resolution enters only as an over-all intensity factor.

1. Resolution Function of the Double Monochromator

The probability that a neutron with angular γ_2 (after the collimator C_2) and energy (Δk_i) deviations from the mean values will get through the double monochromator is

$$I^{(M)} d\gamma_2 d\left(\frac{\Delta k_i}{k_i}\tan\theta_M\right),$$

where

$$I^{(M)}\left(\gamma_2, \frac{\Delta k_i}{k_i}\tan\theta_M\right) = R_M \exp\left\{-\tfrac{1}{2}\left[a_M\gamma_2^2 + 2b_M\gamma_2\frac{\Delta k_i}{k_i}\tan\theta_M + c_M\left(\frac{\Delta k_i}{k_i}\tan\theta_M\right)^2\right]\right\}, \tag{16}$$

$$a_M = \frac{1}{\alpha_0^2}+\frac{1}{\alpha_1^2}+\frac{1}{\alpha_2^2}+\frac{1}{\eta_{M_1}^2}+\frac{1}{\eta_{M_2}^2},$$

$$b_M = \frac{2}{\alpha_1^2}+\frac{1}{\eta_{M_1}^2}+\frac{1}{\eta_{M_2}^2}, \tag{17}$$

$$c_M = \frac{4}{\alpha_1^2}+\frac{1}{\eta_{M_1}^2}+\frac{1}{\eta_{M_2}^2},$$

and subscripts 0, 1, and 2 denote the collimator C_0 mosaic crystals M_1 and M_2, etc. R_M is a flux-dependent normalization factor:

$$R_M \simeq \beta_0 k_i \cot\theta_M \phi(k_i) P_M^2(k_i), \tag{18}$$

where β_0 is the vertical divergence of collimator C_0, $\phi(k_i)$ the energy-dependent neutron flux from the reactor, and $P_M(k_i)$ is the energy-dependent monochromator reflectivity. β_0 enters the expression because the assumption is made that the vertical resolution is dominated by the in-pile collimation.

Integration of (16) over the energy variable gives

$$I_\gamma^{(M)}(\gamma_2) = R_M\left(\frac{2\pi}{c_M}\right)^{1/2}\exp\left[-\tfrac{1}{2}\left(a_M-\frac{b_M^2}{c_M}\right)\gamma_2^2\right]. \tag{19}$$

Since $\alpha_1 \gg \eta_{M_1}, \eta_{M_2}, \alpha_0, \alpha_2$, we have for the angular-divergence width

$$W_\gamma^2 = \left(a_M-\frac{b_M^2}{c_M}\right)^{-1} \simeq \left(\frac{1}{\alpha_0^2}+\frac{1}{\alpha_2^2}\right)^{-1}. \tag{20}$$

Therefore the beam divergence after the double monochromator is independent of the mosaic spreads of the monochromating crystals, and the in-pile collimator and monochromator-to-sample collimator play a symmetric role. The energy resolution can be obtained by integrating equation (16) over the angular variable,

$$I_e^{(M)}\left(\frac{\Delta k_i}{k_i}\tan\theta_M\right) = R_M\left(\frac{2\pi}{a_M}\right)^{1/2} \times \exp\left[-\tfrac{1}{2}\left(c_M-\frac{b_M^2}{a_M}\right)\left(\frac{\Delta k_i}{k_i}\tan\theta_M\right)^2\right]. \tag{21}$$

We again define the energy-width parameter as

$$W_M^{-2} = c_M - b_M^2/a_M \simeq \frac{2}{\eta_M^2}\left(\frac{1}{\alpha_0^2}+\frac{1}{\alpha_2^2}\right)\left(\frac{1}{\alpha_0^2}+\frac{1}{\alpha_2^2}+\frac{2}{\eta_M^2}\right)^{-1}. \tag{22}$$

It is then straightforward to show that, for a given W_M, the intensity $I_e^{(M)}$ is maximized when

$$\frac{2}{\eta_M^2} \equiv \frac{1}{\eta_{M_1}^2}+\frac{1}{\eta_{M_2}^2} \simeq \frac{1}{\alpha_0^2}+\frac{1}{\alpha_2^2}. \tag{23}$$

In other words, the effective mosaic spread of the double-crystal system should match the collimator widths. Under this condition we have the optimized beam divergence of

$$W_\gamma = \tfrac{1}{2}\sqrt{2}\eta_M \tag{24}$$

[from Eq. (20)] and the beam energy width of

$$\Delta E_i = 2(2\ln 2)^{1/2}\eta_M 2E_i \cot\theta_M. \tag{25}$$

Comparison of the above results with the standard single-monochromator resolution function shows that a double-monochromator system behaves like a single-monochromator system with a relaxed in-pile collimator, an equivalent mosaic crystal of spread $\eta_{M_1}\eta_{M_2}/(\eta_{M_1}^2+\eta_{M_2}^2)^{1/2}$, and an equivalent monochromator-to-sample collimator of width $\alpha_0\alpha_2/(\alpha_0^2+\alpha_2^2)^{1/2}$. Under this condition the single monochromator has an optimized beam energy width of $2(2\ln 2)^{1/2}\sqrt{2}\eta_M 2E_i \cot\theta_M$ and beam divergence of $W_\gamma = \eta_M$. Therefore, aside from the loss of intensity due to double monochromation, the double monochromator has a $\sqrt{2}$ factor better energy and directional resolution compared to the single monochromator.

2. Resolution Function of the Analyzer Spectrometer

This is the same as the conventional TAS and the corresponding $I_e^{(A)}$ can be written down as[21]

$$I_e^{(A)}\left(\frac{\Delta k_f}{k_f}\tan\theta_A\right) = R_A\left(\frac{2\pi}{a_A}\right)^{1/2} \times \exp\left[-\tfrac{1}{2}\left(c_A - \frac{b_A^2}{a_A}\right)\left(\frac{\Delta k_f}{k_f}\tan\theta_A\right)^2\right], \tag{26}$$

$$R_A = \beta_A k_f \cot\theta_A P_A(k_f),$$

$$\beta_A = \left(\frac{1}{\beta_3^2} + \frac{1}{\beta_4^2}\right)^{-1},$$

$$a_A = \frac{1}{\alpha_3^2} + \frac{1}{\alpha_4^2} + \frac{1}{\eta_A^2}, \tag{27}$$

$$b_A = -\left(\frac{1}{\eta_A^2} + \frac{2}{\alpha_4^2}\right),$$

$$c_A = \frac{1}{\eta_A^2} + \frac{4}{\alpha_4^2}.$$

The width function W_A is given by

$$W_A^{-2} = c_A - b_A^2/a_A = \frac{1}{a_A}\left[\frac{1}{\alpha_3^2}\left(\frac{1}{\eta_A^2} + \frac{4}{\alpha_4^2}\right) + \frac{1}{\eta_A^2\alpha_4^2}\right]. \tag{28}$$

Under the usual condition $\alpha_4 \gg \alpha_3, \eta_A$, an optimized arrangement is to choose $\alpha_3 \simeq \eta_A$, resulting in

$$W_A \simeq (\alpha_A^2 + \eta_A^2)^{1/2} \simeq \sqrt{2}\eta_A. \tag{29}$$

3. *Energy Resolution Function of TAS*

By the energy resolution function of TAS we mean the energy width measured with a sample which has the following neutron cross section:

$$\frac{d^2\sigma}{d\Omega\, d(\Delta k_f)} = \frac{d^2\sigma}{d\Omega\, d\omega}\frac{d\omega}{d(\Delta k_f)} = \sigma_0\delta\left(\omega - \frac{\hbar}{2m}(k_i^2 - k_f^2)\right)\frac{\hbar}{m}k_f. \tag{30}$$

Solid vanadium is an almost-pure incoherent scatterer and at room temperature approximates closely the above ideal cross section. Therefore, if the thickness of the vanadium plate is t, the quasielastic peak measured with the constant-Q scan would have an intensity distribution

$$I_v(\omega) = \int\int \frac{\hbar}{m}k_f\sigma_0 t\,\delta\left(\omega - \frac{\hbar}{2m}(k_i^2 - k_f^2)\right) \times I_e^{(M)} I_e^{(A)}\, d\left(\frac{\Delta k_i}{k_i}\tan\theta_M\right) d\left(\frac{\Delta k_f}{k_f}\tan\theta_A\right). \tag{31}$$

The integration can easily be done by substituting $I_e^{(M)}$ and $I_e^{(A)}$ from (21) and (26) to obtain

$$I_v(\omega) = (2\pi)^{3/2}\frac{\hbar}{m}\sigma_0 t\frac{R_M R_A}{(a_M a_A)^{1/2}}k_f W_M W_A \frac{2E_f\cot\theta_A}{\hbar^2(W_A^2 + \rho^2 W_M^2)^{1/2}} \times \exp\left[-\frac{1}{2}\frac{\hbar^2\omega^2}{4E_f^2\cot^2\theta_A(W_A^2 + \rho^2 W_M^2)}\right], \tag{32}$$

which is a Gaussian peak with full width at half-maximum,

$$\text{FWHM} = 2(2\ln 2)^{1/2}[2E_f\cot\theta_A\,(W_A^2 + \rho^2 W_M^2)^{1/2}], \tag{33}$$

$$\rho = E_i\cot\theta_M / E_f\cot\theta_A. \tag{34}$$

This means that we can determine the experimental parameters W_m and W_A by use of the vanadium rocking curve with two different combinations of E_i and E_f. For the present experiment, we use an incident energy of $E_i = 12.74$ meV and two vanadium rocking curves were obtained with (002) and (004) planes of the graphite analyzer. The curves were approximately Gaussian with widths of 0.757 and 0.540 meV, from which we then use (33) to obtain the values

$$W_M^{-2} = 82250 \quad \text{and} \quad W_A^{-2} = 64600.$$

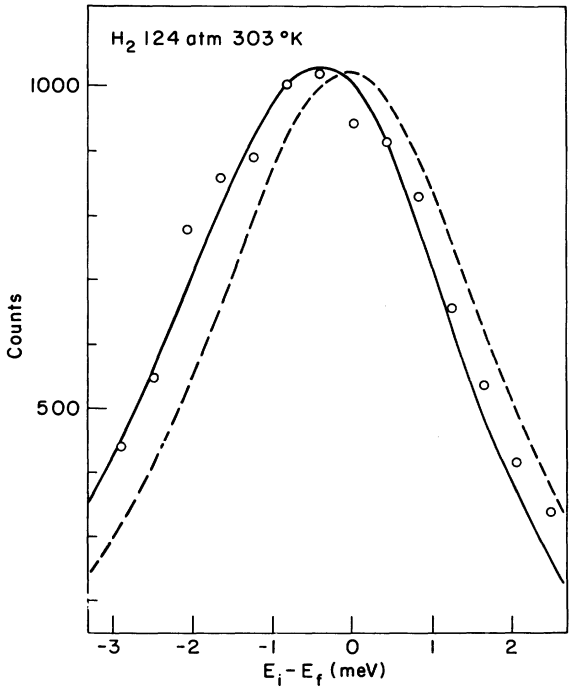

FIG. 2. Illustration of the resolution shift and broadening of the quasielastic peak. The dotted line gives the theoretical curve for a perfect-gas Doppler-broadened cross section corresponding to the temperature. The circles are experimentally measured cross sections and the solid line represents the theoretical cross section convolved with the resolution function. The accuracy of resolution correction can be made to about 5%.

In studying the quasielastic peak of liquids and gases, only the energy resolution function is important. The reason is that the cross section is usually a slowly varying function of Q compared to the momentum resolution function of the spectrometer. In almost all cases the cross section can be considered as a constant over the nonzero range of the momentum resolution function so that its measured value is given by [referring to (32)]

$$\begin{aligned}\sigma_M(Q,\omega) &= \int_{-\infty}^{\infty} I_v(\omega-\omega')\sigma(Q,\omega')\,d\omega' \\ &= (2\pi)^{3/2}\frac{\hbar}{m}P_M^2 P_A \phi(k_i)k_i \cot\theta_M k_f^2 \cot\theta_A \\ &\quad\times \frac{\beta_0\beta_A}{(a_M a_A)^{1/2}}\frac{W_M W_A}{W(\omega)} \\ &\quad\times \int_{-\infty}^{\infty} e^{-(\omega-\omega')^2/2W^2(\omega)}\sigma(Q,\omega')d\omega',\end{aligned} \tag{35}$$

where

$$W^2(\omega) = [(2E_f/\hbar)\cot\theta_A]^2(W_A^2+\rho^2 W_M^2)\,. \tag{36}$$

The important limiting case of (35) is when $\sigma(Q,\omega)$ has a peak much wider than the resolution function. It can then be taken out of the integral. If we assume that the analyzer reflectivity is roughly constant over the region $E_f = 12-15$ meV, and the neutron flux from the reactor is Maxwellian, we have then

$$\sigma_m(Q,\omega) \propto k_i^4 \cot\theta_M k_f^2 \cot\theta_A \sigma(Q,\omega) \tag{37}$$

or

$$\sigma_m(Q,\omega) \propto k_i^3 \cot\theta_M k_f^3 \cot\theta_A S_s(Q,\omega)\,. \tag{38}$$

The hydrogen scattering law has been measured at room temperature and at a pressure of 124 atm with TAS at $Q = 0.3$ Å^{-1}. At this condition $S_s(Q,\omega)$ should be given by the well-known free-particle expression (12). Figure 2 shows the measured points and the theoretical curves with or without the resolution correction of (38). The good agreement substantiates the assumption that the analyzer reflectivity can indeed be taken to be constant over the narrow frequency range of the incoherent peak.

Summarizing the above discussion, we can concisely put the resolution function of the TAS for the present experiment as follows: The resolution function $R(\bar{\omega})$ at an average energy transfer $\hbar\bar{\omega}$ consists of two factors,

$$R(\bar{\omega}) = R_0(\bar{\omega})R_1(\bar{\omega})\,,$$

where $R_0(\bar{\omega})$ is a slowly varying factor equal to

$$R_0(\bar{\omega}) = \bar{k}_f^2 \cot\bar{\theta}_A/[k_f^2\cot\theta_A]_B \tag{39}$$

and the index B means that the value is taken at the Bragg position for which $\bar{\omega}=0$. On the other hand, $R_1(\bar{\omega})$ is a sharp Gaussian function

$$R_1(\bar{\omega}) = [(2\pi)^{1/2}W(\bar{\omega})]^{-1}e^{-\bar{\omega}^2/2W^2(\bar{\omega})}, \tag{40}$$

with an energy-dependent width given by

$$W(\omega) = (2\bar{E}_f/\hbar)\cot\bar{\theta}_A[W_A^2+\rho^2W_M^2]^{1/2}\,. \tag{41}$$

The measured differential cross section is then the convolution of the theoretical cross section and the resolution function, i.e.,

$$\frac{d^2\sigma_m(\bar{\omega})}{d\Omega\,d\bar{\omega}} = R_0(\bar{\omega})\int_{-\infty}^{\infty} R_1(\omega'-\bar{\omega})\frac{d^2\sigma(\omega')}{d\Omega\,d\omega'}\,d\omega'\,. \tag{42}$$

C. Sample and Sample Holder

Two series of measurement have been carried out at pressures of 35, 70, 140 atm and 110, 120, 130 atm, respectively. In both cases the temperature was maintained at 85 ± 1°K. Values of wave-vector transfer Q range from 0.2 to 0.6 Å^{-1}. Above $Q = 0.6$ Å^{-1} the low peak intensity made the measurement inaccurate, and also the y parameter is so small that from the theoretical point of view they are uninteresting. The sample holders were made of 6061-T6 aluminum with cylindrical bore of $1\frac{1}{2}$ in. high by $\frac{1}{4}$ in. diameter. The wall thickness is $\frac{1}{8}$ in. Hydrogen gas used was of research grade with 99.999% purity. The background was measured between experiments at different pressures with the empty sample holder. At the smallest Q the background was found to be fairly sharply peaked at the elastic position.

In data corrections the effects of multiple scattering and self-shielding must be considered. Although our sample holder is a long and rather thin cylinder, the sample transmission is down to about 60% at the highest gas density ($n = 1.09 \times 10^{22}$ cm^{-3}). An estimate of the twice-scattered contribution in this case gives about 40% of the once-scattered intensity.[23] However, the multiply scattered neutrons should have a much broader energy distribution. For example, neutrons scattered into the axial direction have to experience at least two 90° scatterings if they are to arrive at the detector, and with each large-angle scattering considerable broadening will result. The self-shielding correction takes into account those once-scattered neutrons which fail to arrive at the detector because of subsequent multiple scattering in the sample. The effect of this correction is to multiply the measured intensity by an essentially constant factor.[23] Since we are interested in the line shape of the quasielastic peak where $k_0 \simeq k$, we assume corrections can be taken into account approximately by first subtracting the background

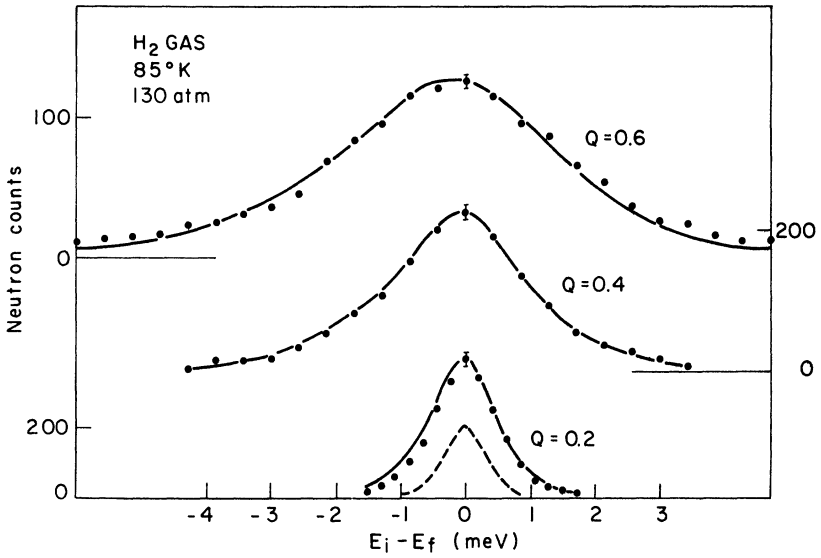

FIG. 3. Measured double differential cross section of hydrogen gas at 85°K and 130 atm. Measurement is done with the constant-Q scan. The dotted curve in the bottom is roughly the resolution width of the spectrometer. The solid lines are the fitted curves with the single-relaxation-time model with variable-α parameter. The experimental linewidths are extracted this way for convenience. As shown in the graph the asymmetry factor has been taken out so that the peaks are centered around $\omega = 0$.

due to the empty sample holder and then subtracting the additional broad background due to multiple scattering. In making these corrections we are also guided by the property that $S_s(Q, \omega)$ should have unit area at any value of Q and that it is given by (12) in the dilute-gas limit $y \ll 1$.

V. DATA ANALYSIS

To analyze the data we calculate $S_s(Q, \omega)$ by solving the linearized Boltzmann equation (6) and apply (11). The result is inserted into the cross-section expression (15), which is then convolved with the experimental resolution function according to (42). Actually what was done was to use the single-relaxation-time-kinetic-model solution[13] to fit the data by using the collision frequency α as a fitting parameter. From the best fit to the experimental line shape we then extracted the *experimental linewidth* of the $S_s(Q, \omega)$. The kind of fit we obtained is typically what is shown in Fig. 3 for the 130-atm data. We judged that this was an accurate and satisfactory way of extracting the experimental linewidth, although the parameter α we thus got may have no physical significance. This procedure gives a value for FWHM at a particular density and wave-number transfer Q. Figure 4 shows the extracted FWHM in meV as a function of Q^2 for pressures 110, 120, and 130 atm. The solid lines are the FWHM of the measured peaks and the dotted lines are the extracted FWHM of $S_s(Q, \omega)$. In order to compare this with theory we like to take into account the scaling property of the linearized Boltzmann equation. Namely, the $S_s(Q, \omega)$ calculated from the equation is really a function of reduced variables, $x = \omega/\sqrt{2}Qv_0$, and the collision parameter y alone. It is more general and convenient to define y as $v_0/\sqrt{2}DQ$, which is also consistent with the previous definition $\alpha/\sqrt{2}Qv_0$ which is applicable to the single-relaxation-time model. Then the problem is to determine D as a function of density. In the case of the hard sphere the self-diffusion coefficient is related to the hard-sphere diameter and the gas density by[24]

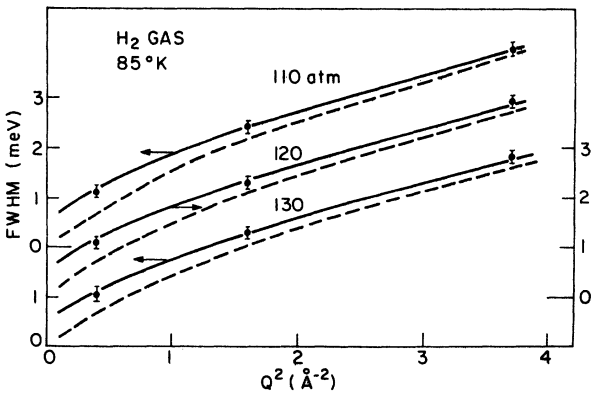

FIG. 4. This figure shows the linewidth as a function of Q^2. The solid line gives the linewidth of the measured $S_s(Q,\omega)$ as, for example, given in Fig. 3. The dotted line gives the extracted linewidths after deconvolution.

$$D=1.019(\tfrac{3}{8})(k_BT/\pi m)^{1/2}(n\gamma_0^2)^{-1}, \quad (43)$$

which is valid at low densities. For a dense gas, such as we have, we should apply the Enskog correction, which gives the diffusion coefficient at higher density n in terms of the one at lower density n_0 according to

$$D(n)=D(n_0)(n_0/n)\chi^{-1}, \quad (44)$$

where

$$\chi=1+0.625(\tfrac{2}{3}\pi n\gamma_0^3)+0.2869(\tfrac{2}{3}\pi n\gamma_0^3)^2 +0.115(\tfrac{2}{3}\pi n\gamma_0^3)^3 \quad (45)$$

is the dimensionless excess compressibility factor for a hard-sphere fluid.

This factor ranges from 1.07 for the pressure at 35 atm ($n=3.08\times10^{21}$ cm^{-3}) to 1.28 at 140 atm ($n=1.09\times10^{22}$ cm^{-3}). We take as the reference density $n_0=8.8\times10^{19}$ at 1 atm, for which the value of D is 0.172 cm^2/sec at 85 °K.[25] It should be noted that a recent computer molecular-dynamics experiment[26] indicates that the Enskog prediction underestimates the self-diffusion coefficient because the collective effects in the fluid which lead to persistent correlation have been ignored. The enhancement effect has been observed in the self-diffusion coefficient measurements on methane[27] and krypton.[28] This means that our calculation of D based on (44) could be somewhat lower than the true values. Judging from the computer molecular-dynamics result on a hard-sphere gas[26] we estimate that this enhancement correction to D is not more than 10% at 140 atm and is correspondingly smaller at lower pressures.

Figure 5 shows the reduced FWHM plotted against y. The experimental points are shown as black dots; and the theoretical prediction is represented by the solid line. The theoretical curve is made up of the hard-sphere calculation of Mazenko, Wei, and Yip[10] and hard-sphere, Lenard-Jones, and exp-6 potential calculations of Desai[29] (the latter calculations are represented, respectively, as crosses, triangles, and squares in the graph). We note that various calculations using widely different potentials give more or less the same FWHM.

VI. DISCUSSIONS

There are two ways of solving Boltzmann-type kinetic equations to obtain $S_s(k\omega)$. One way is to use the kinetic equation to compute the mean-square displacement function $\langle r^2(t)\rangle$ and higher-

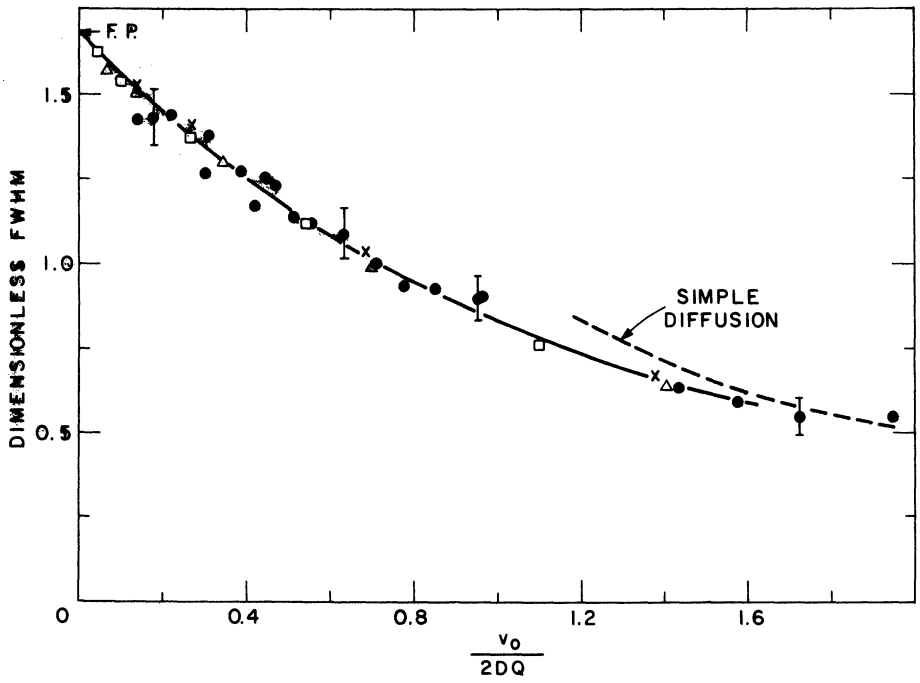

FIG. 5. Dimensionless FWHM of $S_s(Q,\omega)$ plotted against the y parameter for all the measurements. The dimensionless FWHM is defined as the FWHM of Fig. 4 divided by Qv_0 and $y\equiv v_0/2DQ$. In this plot v_0 is taken as $(2k_BT/m)^{1/2}$, which is different from the definition in the text by factor $\sqrt{2}$. The black points are experimental values; the solid line is the hard-sphere calculation of Mazenko, Wei, and Yip (Ref. 10); and the crosses, triangles, and squares are calculations of Desai (Ref. 28) for hard-sphere, Lenard-Jones, and exp-6 potentials, respectively. Also indicated are the known limiting cases of free particles and simple diffusion.

order spacial moments of $G_s(r,t)$. Non-Gaussian corrections to the Gaussian approximation can be calculated in terms of $\langle r^{2n}(t)\rangle, n \geq 2$. This is the approach used by Desai.[29] The other method of calculating $S_s(k\omega)$ is based on the use of generalized kinetic models.[30] This method has been used by Mazenko *et al.*[10] The hard-sphere result of Mazenko *et al.* agrees numerically with the hard-sphere result of Desai. So one has confidence in both methods of calculations. Desai's method is more flexible in that it can handle the other potentials more easily. But the same method would not work for the full density correlation function since in this case the Gaussian approximation is not good. On the other hand, the kinetic-model method is equally well suited for $G_s(r,t)$ as well as $G(r,t)$ problems. For example, the generalized Boltzmann equation for hard spheres has been treated in this way by Mazenko *et al.*[10]

As we remarked earlier the reduced FWHM computed using the different potentials differ only slightly. This indicates that the spectral distribution of $S_s(k\omega)$ is not sensitive to the details of the short-range interaction between molecules. By details we mean the steepness of the repulsive part of the interaction as well as the presence of a long-ranged attractive tail. In addition, a softer repulsive interaction, the Maxwell potential, has been studied recently by Deutsch.[31] The FWHM values also fell into the same theoretical curve of Fig. 5. It appears that in order to learn anything about the details of the interaction potential we will have to study the van-Hove self-correlation function over a wide range of temperatures. It is interesting to note that the present data on FWHM enables us to distinguish between direct calculations using the Boltzmann equation itself and the model solutions. Although not indicated in Fig. 5, a comparison between the present data and the former calculation[12] using the one-relaxation-time model[13] shows that the model could be off by about 5% for values of $y \sim 1.0$. The single-relaxation-time model assumes that the collisions are very effective in thermalizing the velocity distribution of the molecules, which results in an underestimate of the FWHM. At the opposite extreme the Fokker-Planck approximation[32] assumes grazing collisions and small changes in the particle velocities and it gives an overestimate of FWHM of about the same magnitude.[31] The accuracy of kinetic-model approximation improves markedly if a few more eigenvalues of the collision operator (or, equivalently, the relaxation times) are considered explicitly. For example, a three-relaxation-time model gives result accurate to 0.66% in the case of Maxwell molecules.[31] Thus in some sense one is seeing from the data the effects of a distribution of relaxation times.

In conclusion we have demonstrated the effects of collisional narrowing in a gas by means of a neutron scattering experiment. It may be surprising that the lineshape observed with such a high-frequency and large-wave-number probe can be quantitatively explained by using kinetic theory based on the Boltzmann equation. We believe that the good agreement obtained is rather special to the case of single-particle motion. On theoretical grounds one can show that at least in the case of a low-density hard-sphere fluid the Boltzmann equation is correct at all frequencies and wavelengths. It would be most interesting to extend this kind of measurements to $S(k\omega)$, the full density correlation spectra. There we expect that the Boltzmann equation would break down and one needs to use the generalized kinetic equation derived by Mazenko.[8] Even with the measurement of $S_s(k\omega)$, we think that at sufficiently high density, such that $\eta > 0.2$, we should begin to see the collective enhancement effect of D, as was observed by the computer molecular dynamics.[26]

ACKNOWLEDGMENTS

One of us (S.Y.) is grateful to the John Simon Guggenheim Memorial Foundation for a Fellowship in 1972-73. He also would like to acknowledge the hospitality of the Physics Department, Harvard University during this period.

---

*Research supported by contract AEC AT(11-1) 3352.

[1]For review, see B. J. Berne and D. Forster, Ann. Rev. Phys. Chem. 22, 563 (1972).

[2]G. F. Mazenko, Phys. Rev. A 1, 209, 222 (1970).

[3]See, for example, D. Forster and P. C. Martin, Phys. Rev. A 2, 1575 (1970).

[4]G. E. Uhlenbeck and G. W. Ford, *Lectures in Statistical Mechanics* (American Mathematical Society, Providence, R. I., 1963).

[5]E. G. D. Cohen, in *Fundamental Problems in Statistical Mechanics*, edited by E. G. D. Cohen (North-Holland, Amsterdam, 1962).

[6]S. Yip, J. Acoust. Soc. Am. 49, 941 (1971).

[7]B. J. Alder and T. E. Wainwright, Phys. Rev. Lett. 18, 988 (1967).

[8]G. F. Mazenko, Phys. Rev. A 3, 2121 (1971); 5, 2545 (1972).

[9]C. D. Boley, Phys. Rev. A 5, 986 (1972).

[10]G. F. Mazenko, T. Wei, and S. Yip, Phys. Rev. A 6, 1981 (1972).
[11]H. H. U. Konijnendijk and J. M. M. Van Leeuwen, Physica 64, 342 (1973).
[12]Y. Lefevre, S. H. Chen, and S. Yip, *Neutron Inelastic Scattering* (IAEA, Vienna, 1972), p. 445.
[13]M. Nelkin and A. Ghatak, Phys. Rev. 135, A4 (1964).
[14]R. C. Desai and M. Nelkin, Nucl. Sci. Eng. 24, 142 (1966).
[15]A. Z. Akcasu and J. J. Duderstadt, Phys. Rev. 188, 479 (1969).
[16]L. van Hove, Phys. Rev. 95, 249 (1954).
[17]V. F. Sears, Proc. Phys. Soc. Lond 86, 965 (1965).
[18]O. Eder, S. H. Chen, and P. A. Egelstaff, Proc. Phys. Soc. Lond. 89, 833 (1966).
[19]R. Aamodt, K. M. Case, M. Rosenbaum, and P. F. Zweifel, Phys. Rev. 126, 1165 (1962).
[20]R. Stedman, L. Almquist, G. Raunio, and G. Nilsson, Rev. Sci. Instrum. 40, 249 (1969). We are grateful to Dr. Stedman for sending us blueprints of his original design.
[21]Y. Lefevre, Ph.D. thesis (MIT, 1972) (unpublished).
[22]M. J. Cooper and R. Nathans, Acta Cryst. 23, 357 (1967).
[23]J. Copley (private communications). We are grateful to Dr. Copley for supplying us with a graph of unpublished calculations on multiple scatterings.
[24]S. Chapman and T. G. Cowling, *The Mathematical Theory of Non-Uniform Gases* (Cambridge U. P., New York, 1953).
[25]*American Institute of Physics Handbook*, 2nd ed. (McGraw-Hill, New York, 1963), p. 2-236.
[26]B. J. Alder, D. M. Gass, and T. E. Wainwright, J. Chem. Phys. 53, 3813 (1970).
[27]N. J. Trappeniers and P. H. Oosting, Phys. Rev. 51, 418 (1971).
[28]P. Carelli, I. Modena, and F. P. Ricci, Phys. Rev. A 7, 298 (1973).
[29]R. C. Desai, Ph.D. thesis (Cornell University, 1966) (unpublished); J. Chem. Phys. 44, 77 (1966).
[30]E. P. Gross and E. A. Jackson, Phys. Fluids 2, 432 (1959); A. Sugawara, S. Yip, and L. Sirovich, Phys. Fluids 11, 925 (1968).
[31]O. L. Deutsch, M.S. thesis (MIT, 1973) (unpublished).
[32]S. Yip and Ranganathan, Phys. Fluids 8, 1956 (1965).